

# LOCAL STRUCTURE AND CHEMICAL BONDING IN PRECURSOR-DERIVED AMORPHOUS CERAMICS

Hui GU

Ceramics Superplasticity Project, ICORP, Japan Science and Technology Corporation, JFCC  
2F, 2-4-1 Mutsuno, Atsuta, Nagoya 456-8587  
E-mail: gu@ngo.jst.go.jp

## ABSTRACT

The structural and chemical properties of the precursor-derived amorphous materials were studied using the advanced methods and full power of the analytical electron microscopy, including quantitative electron energy-loss spectroscopy (EELS) analysis, energy-loss near-edge structures (ELNES) analysis, high-resolution electron microscopy (HREM) imaging, high-angle annular dark-field (HADF) Z-sensitive imaging and finally EELS/ELNES spectrum-imaging technique. Three materials systems were investigated in details: (a) Si-B-C-N system, (b) Si-C-N system and (c) Si-C-O system. It is always found that the chemical composition and bonding are not homogeneous at the scale of 1 to several nanometers, even the amorphous matrix appears uniform down to atomic level in Si-(B)-C-N systems.

In Si-B-C-N system, clusters of 1-3 nm size were observed by HADF imaging directly. These clusters are rather stable at temperatures at least up to 1600 °C. EELS quantification reveals that the composition in the amorphous monolith has little changed by high temperature deformation. ELNES results indicated not only that these clusters are embedded in graphite-like carbon "matrix" but Si-N bonds dominate in the clusters. It is believed that the addition of boron prohibited the Si-N clusters to grow at high temperature.

In Si-C-N system the situation is very similar except the crystallization took place at temperature several 100 °C lower. The clusters are very much like Si<sub>3</sub>N<sub>4</sub> in chemical bonding from ELNES result, and EELS quantification indicated the same thing. But their structure remained amorphous. The amount of carbon is substantially less than in Si-B-C-N monolith, it is more like amorphous carbon than graphite-like, according also to ELNES.

In Si-C-O system crystalline SiC clusters were always found regardless of the oxygen content and of the pyrolysing ( $\geq 1300$  °C so far) and annealing temperatures. Instead, their size and abundance vary with these parameters. Graphite was also observed everywhere. ELNES analysis clearly identified that the remaining amorphous structures are made from SiO<sub>2</sub> and carbon. EELS and ELNES profiles exhibited clearly the spatial variation of composition and chemical bonding in consistent completely with such picture.

The common observation of clusters, amorphous or crystalline, reflects fundamental properties of precursor-derived ceramic materials. It is phase separation in amorphous state at 1 nm scale. This remarkable property is a result of absence of atom diffusion in amorphous monolith. Such a new and stable structure is based not only on zero diffusivity but also on the inflexibility of covalent bonds in amorphous state, in stark contrast with the flexibility of amorphous SiO<sub>2</sub>. This observation raises the prospect of forming uniform covalent amorphous that should be more elastic and fracture resistant.

## 1. INTRODUCTION

Ceramic materials derived from polymer precursors opened a new chapter for material processing and engineering [1, 2]. Such new processing route enables the architectural designing from the molecular units level, thus it is expected to be able to control the local structures and therefore, the desired mechanical properties of the advanced ceramics. This processing includes a key step of pyrolyzation to ceramitize the forged and pressed organic polymers, therefore avoids the traditional way of sintering at high temperature. However the thermodynamic equilibrium has not been achieved through large scale atomic displacements, therefore amorphous phase usually remains after pyrolysis. To understand the structural and chemical properties of such pyrolysed materials will provide key information to understand the behavior of such new materials.

Modern analytical electron microscopy has been proved useful to tackle this problem. EELS analysis can give us chemical composition, and ELNES study provides information about coordination and chemical bonding. Combined with a small electron probe from a scanning transmission electron microscope (STEM) we can also obtain the spatial distribution of these information down to atomic scale. Besides, HREM imaging and HADF imaging in STEM enable us directly see the structure, ordering and even chemically sensitive phenomenon. In this work, A STEM (VG-HB601UX-R2) equipped with an EELS spectrometer (Gatan DigiPEELS 766) was the main instrument. It can provide an electron probe as small as 2.5 Å and an energy resolution better than 0.5 eV. HREM observation was undertaken using a Jeol 2010 microscope of JFCC. The EELS “spectrum-imaging” package has been installed in STEM (CNRS-University Paris-Sud/JST-Nanutube). This function enables the synchronized operation of STEM and EELS, thus brings the best out of both parts and greatly improves the performance of analysis.

Three materials systems were analyzed, Si-B-C-N, Si-C-N and Si-C-O systems. The results are given in the three sub-sections respectively in the results section .

## 2. RESULTS

### 2.1 Si-B-C-N

Although the structure of the pyrolysed monoliths is amorphous as shown in HREM image of Fig. 1, STEM images revealed cluster structure in the amorphous matrix in the dimension of 1-3 nm, as presented in Fig. 2. Bright-field (BF) STEM image also shows many tiny pieces of graphite with sizes in the same range or smaller. Boron has successfully entered the matrix of monolith as revealed in the EELS spectrum (Fig. 3).

Upon annealing and deformation at temperature as high as 1600 °C, these clusters remained and their size has little increased. EELS quantification indicates also that the composition of amorphous monolith did not changed in any significant way either. The cluster picture and their sizes provide supports for explaining the high temperature deformation behavior especially the hardening [3].

ELNES results give further information about the largely amorphous structure. As shown in Fig. 4a, carbon ELNES of Si-B-C-N is remarkably similar to that of graphite which agrees with the STEM observation in Fig. 2. On the other hand, nitrogen ELNES exhibits similarity with Si<sub>3</sub>N<sub>4</sub> as seen in Fig. 4b. Si ELNES also indicates Si-N bonds instead of Si-C bonds (not shown). It is therefore clear that there are separately Si-N and graphite “phase” zones in amorphous Si-B-C-N matrix. It is only possible that the observed clusters are made of Si-N

phase but not graphite, because not only Si-N phase should have a higher density than carbon therefore appear brighter in HADF image, but also the graphite zone has different shape as the clusters as seen in STEM BF image.

Boron has certainly prevented diffusion at elevated temperature since Si-B-C-N amorphous structure can be maintained at higher temperature than Si-C-N. However, it is not known yet whether it stays in one of the “phases” or at the frontiers of these zones. From the work of grain boundary analysis in boron-doped SiC nanocrystalline materials, it is found that boron and carbon formed stable interfacial structure [4, 5, 6]. This may still be the case although further prove is necessary from boron ELNES. However, boron could only be connected to either carbon or nitrogen. For B-N bond there is a characteristic feature in nitrogen ELNES [7, 8]. This feature cannot be seen in Fig. 4b although boron content is still a quarter of nitrogen content, an indication that usual B-N bonds did not exist in Si-B-C-N.

## 2.2 Si -C-N

In Si-C-N, the amorphous matrix remained. So did the cluster structure. With the lack of boron the amorphous phase is no longer stable at around 1400 °C. EELS analysis indicated that the Si:N ratio became very close to the same as 3:4 in Si<sub>3</sub>N<sub>4</sub>. Its spectrum is also shown in Fig. 3 along with Si-B-C-N.

Indeed the nitrogen ELNES result of Si-C-N exhibits identical features as that of Si<sub>3</sub>N<sub>4</sub> (also in Fig. 4b). For carbon its amount is substantially less than in Si-B-C-N, as can be seen in Fig. 3. Comparison of carbon ELNES of Si-C-N with the references reveals that carbon structure is more close to amorphous than graphite (Fig. 4a). The state of carbon zones may also be a factor to influence the stability of the Si-N clusters.

HIPing at 1500 °C already made Si-C-N amorphous monolith transformed into multi-phase composite with  $\alpha$ -Si<sub>3</sub>N<sub>4</sub>, graphite and amorphous SiO<sub>2</sub> as the major, secondary and minor phases, respectively [9]. This is in agreement with the thermodynamic calculation of the final phase equilibrium at this temperature [3, 10].

## 2.3 Si-C-O

Precursor-derived Si-C-O materials gives a different situation to compare with Si-(B)-C-N since Si-N cluster is no longer presented here. Three samples with different pyrolysis temperatures and oxygen contents were investigated, PCS-13 with no oxygen and pyrolysed at 1300 °C, PCS10-15 with 16 wt% oxygen at 1500 °C, and PCS10-13 with 22 wt% at 1300 °C. All three samples have crystalline SiC cluster and graphite zones, both in the nanometer order. However, the size of SiC particles are different, from as big as 8-10 nm in PCS-13 to as small as 2-4 nm in PCS10-15 and in PCS10-13. The latter is similar to the size of amorphous Si-N clusters in Si-(B)-C-N. HREM image of PCS10-13 is shown in Fig. 5. Amorphous structure was also visible in those samples, but it is much less in PCS-13 than in the other two. This implies that the remaining amorphous may be SiO<sub>2</sub>.

Indeed ELNES analysis of silicon indicates that there is SiO<sub>2</sub> phase in PCS10-13 and PCS10-15 besides SiC phase, while there is only SiC in PCS-13. Both cases were shown in Fig. 6a together with SiO<sub>2</sub> and SiC references. Therefore SiO<sub>2</sub> phase is definitely contained in the remaining amorphous zones and carbon may also be a part. Carbon ELNES of these samples are shown in Fig. 6b with SiC and graphite. It is interesting to notice that nano size SiC clusters have lost some of the fine features in the bulk SiC.

EELS and ELNES profiles of both PCS-13 and PCS10-13 do exhibit the spatial variation of composition and chemical bonding in accordance with the above results. In Fig. 7a, silicon

profile in PCS-13 follows the contrast in HADF while carbon profile has the opposite variation. This indicates that the amount of graphite is higher than the amount of carbon in SiC, and graphite does have less contribution to HADF than SiC, as speculated in Si-B-C-N case. For PCS10-13, the situation is not so simple as the clusters are smaller, the sample thickness is not uniform, and there were also oxygen (Fig. 7b). Separating contributions of carbon from pure carbon and carbon in SiC clusters, it yields two corresponding carbon profiles, one follows the trends in Si profile, the other against them.

An important message came from these results: the amorphous phases play a key role in prohibiting cluster growth, while the temperature does not have a strong effect in this aspect. This is a common assessment with Si-(B)-C-N systems also the exact mechanism, phases, structures are all different.

### 3. CONCLUSION

The common observation of clusters, amorphous or crystalline, reflects fundamental properties of precursor-derived ceramic materials. It is phase separation in amorphous state at 1 nm scale. This remarkable property is a result of absence of atom diffusion in amorphous monolith. Such a new and stable structure is based not only on zero diffusivity but also on the inflexibility of covalent bonds in amorphous state, in stark contrast with the flexibility of amorphous SiO<sub>2</sub>. This observation raises the prospect of forming uniform covalent amorphous that should be more elastic and fracture-resistant.

### REFERENCES

- [1] J. Bill and F. Aldinger, "Precursor-derived covalent ceramics", *Adv. Mater.*, **7** 775-787 (1995).
- [2] R. Riedel, A. Kienzle, W. Dressler, L. Ruwisch, J. Bill and F. Aldinger, "A silicon carbonitride ceramic stable to 2000 °C", *Nature*, **382** 796-798 (1996).
- [3] B. Baufeld, H. Gu, J. Bill, F. Wakai and F. Aldinger, "High temperature deformation of precursor-derived amorphous Si-B-C-N ceramics", *J. Euro. Ceram. Soc.*, in press (1999).
- [4] H. Gu, Y. Shinoda and F. Wakai, "Detection of boron segregation to grain boundaries in silicon carbide by spatially resolved electron energy loss spectroscopy", *J. Am. Ceram. Soc.*, **82** 469-472 (1999).
- [5] H. Gu, Y. Shinoda, "Structural and chemical widths of general grain boundary in  $\beta$ -silicon carbide: modification of local bonding by boron", *Interface Science*, in reviewing.
- [6] H. Gu, "Stable and unstable grain boundary structures in nanocrystalline SiC", this proceedings.
- [7] Y. Zhang, H. Gu, K. Suenaga and S. Iijima, "Heterogeneous growth of B-C-N nanotubes by laser ablation", *Chem. Phys. Lett.*, **279** 264-269 (1997).
- [8] Y. Zhang, H. Gu and S. Iijima, "Single-wall carbon nanotubes synthesized by laser ablation in a nitrogen atmosphere", *Appl. Phys. Lett.*, **73** 3827-3829 (1998).
- [9] Ishihara, this proceedings.
- [10] M. Weinmann, J. Schuhmacher, H. Kummer, S. Prinz, J. Peng, H. J. Seifert, M. Christ, K. Müller, J. Bill and F. Aldinger, "Synthesis and thermal behavior of novel Si-B-C-N ceramic precursor", *Chem. Mater.*, submitted.

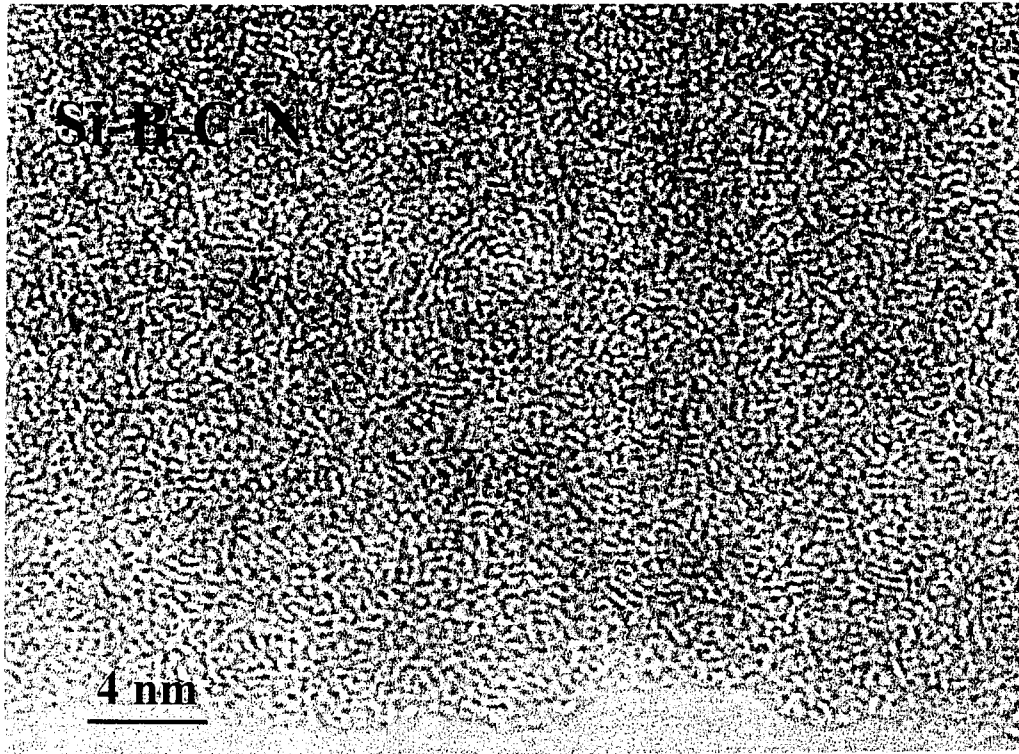


Fig. 1 HREM image of the amorphous structure in precursor-derived Si-B-C-N.

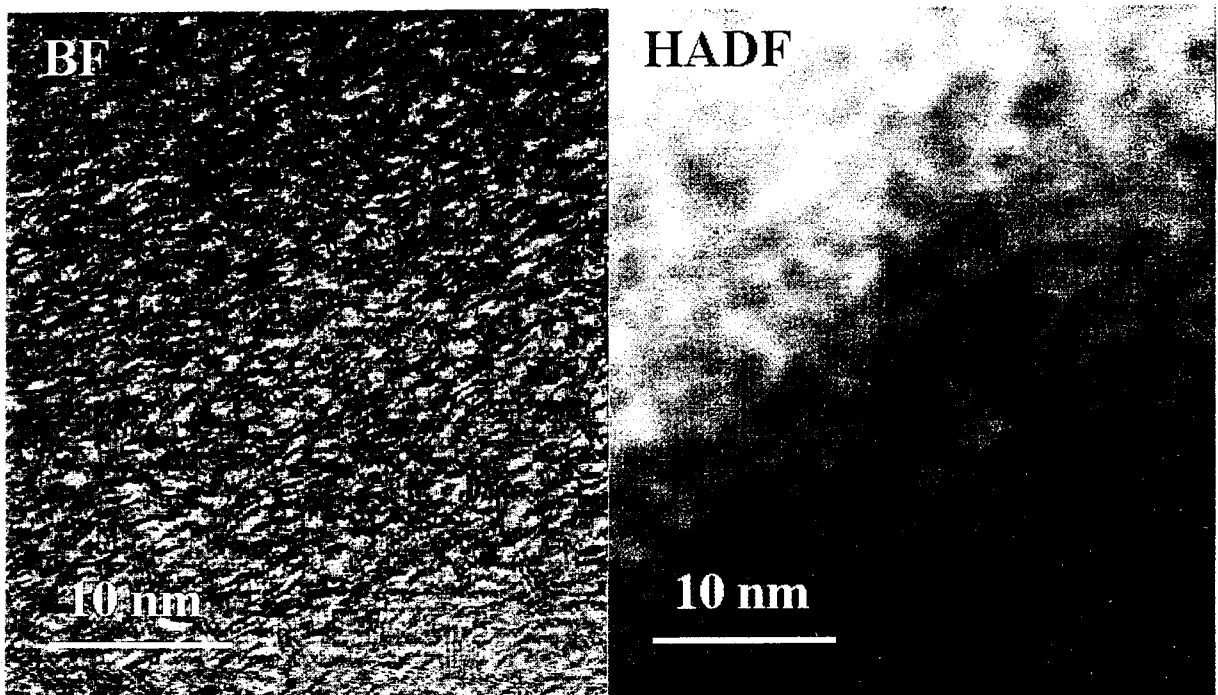


Fig. 2 STEM image of amorphous Si-B-C-N. *Left:* BF image revealed graphite pieces of half to several nanometers. *Right:* HAADF image of clusters of 1-3 nm size.

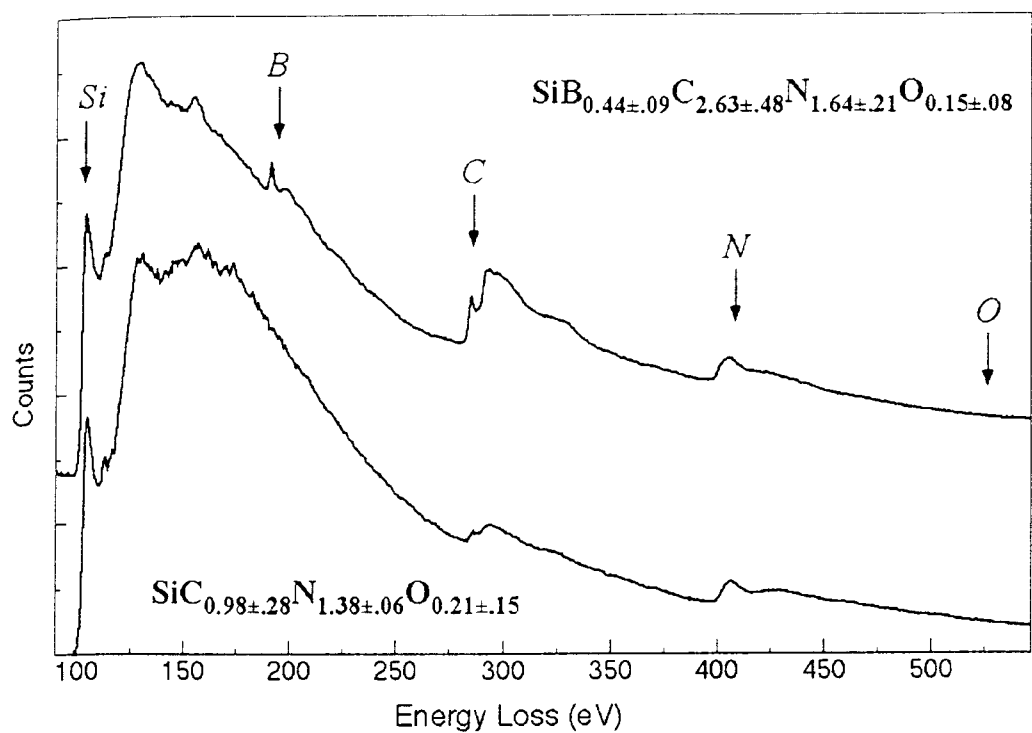


Fig. 3 EELS spectra of Si-B-C-N (upper) and Si-C-N (lower) materials. Their average compositions are given in the figure.

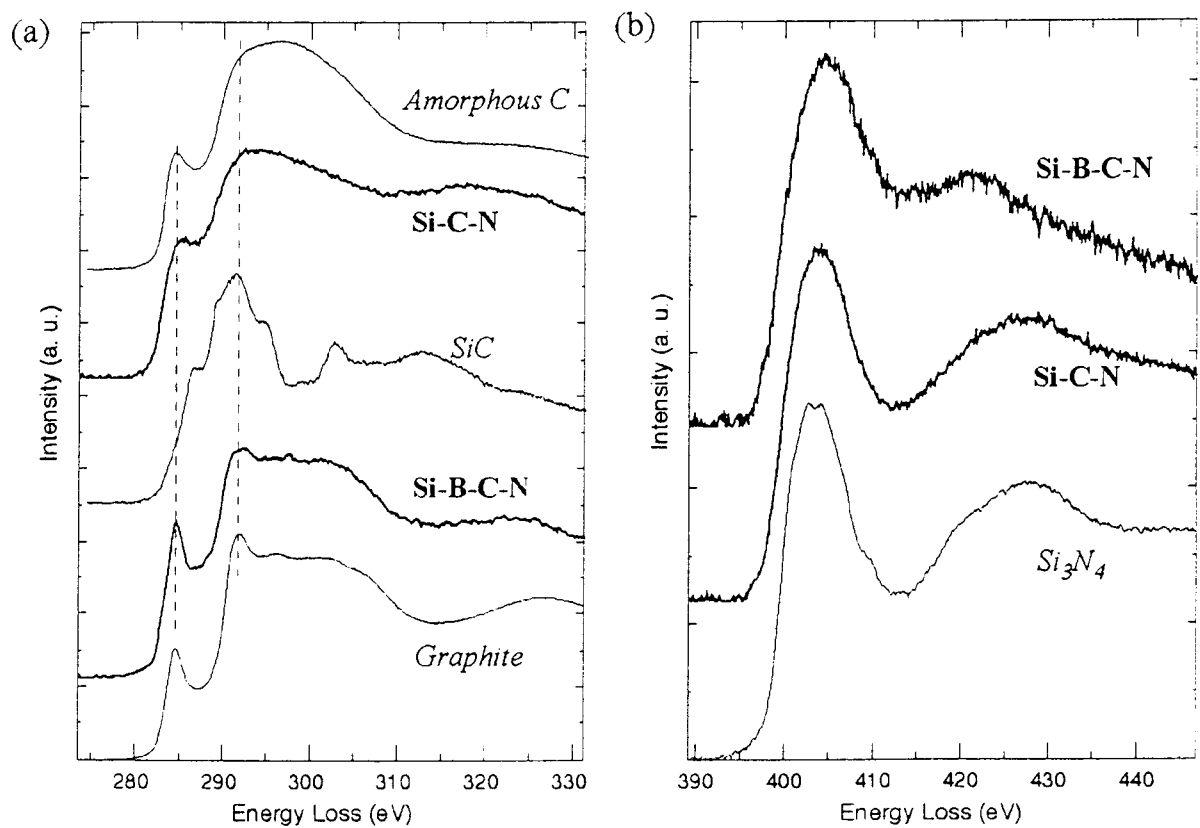


Fig. 4 ELNES of Si-B-C-N and Si-C-N with references: (a) carbon, (b) nitrogen.

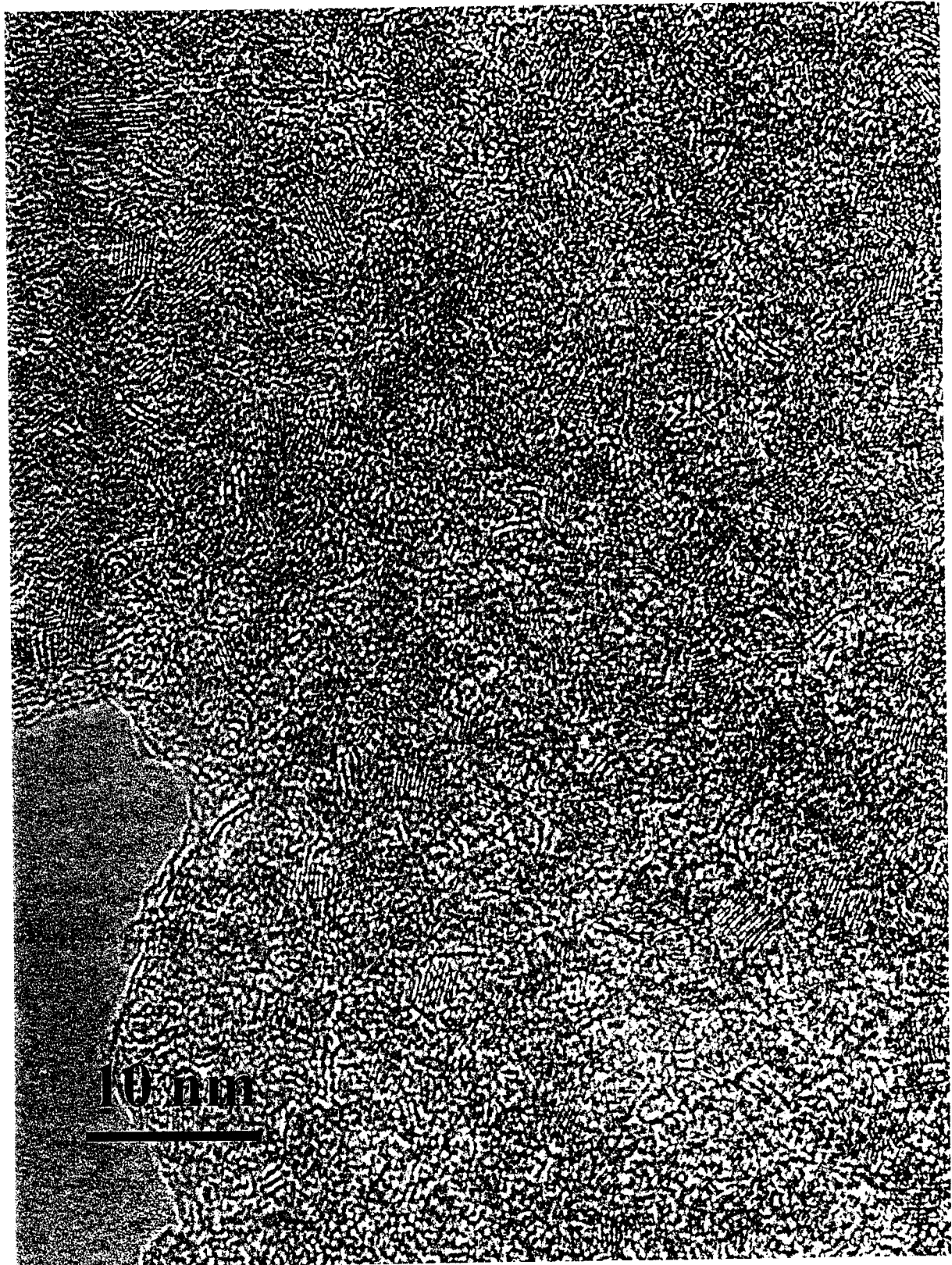


Fig. 5 HREM image of precursor-derived Si-C-O (PCS10-13) showing SiC particles.

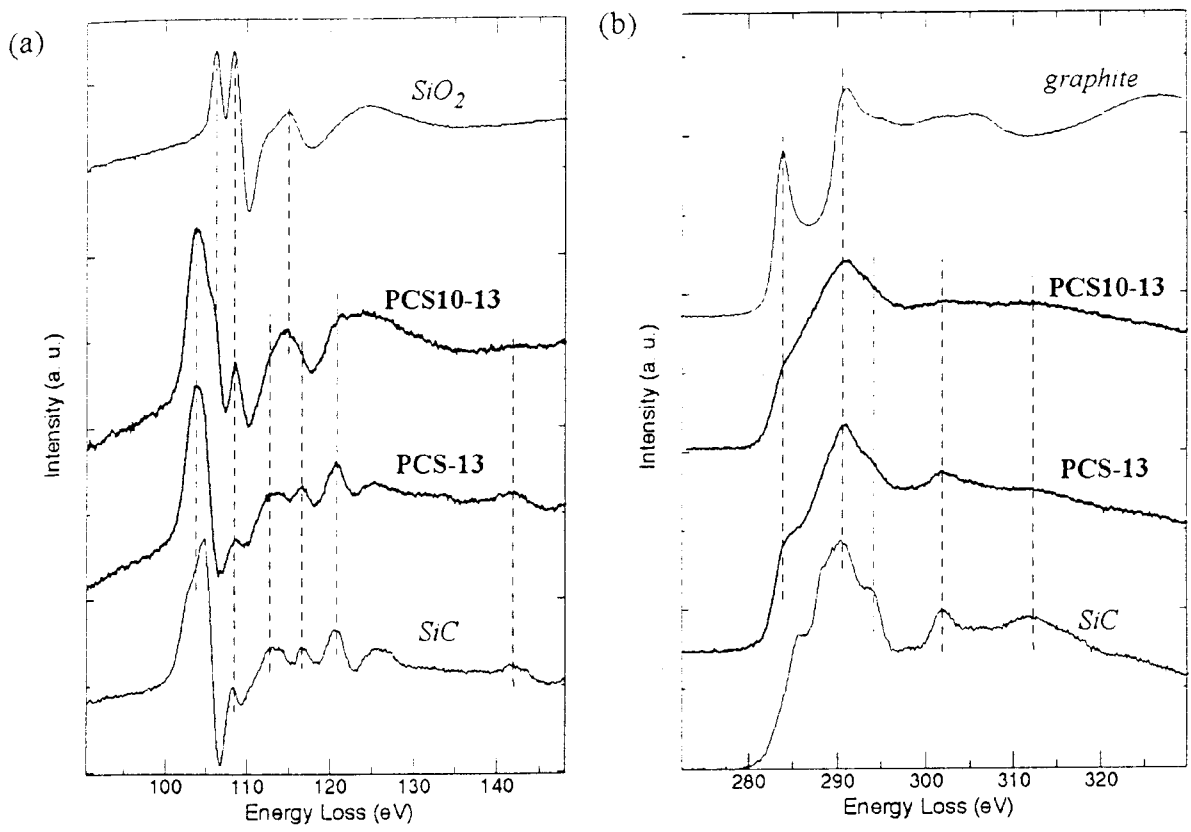


Fig. 6 ELNES of Si-C-(O) with references: (a) Si ELNES in derivative form, (b) carbon.

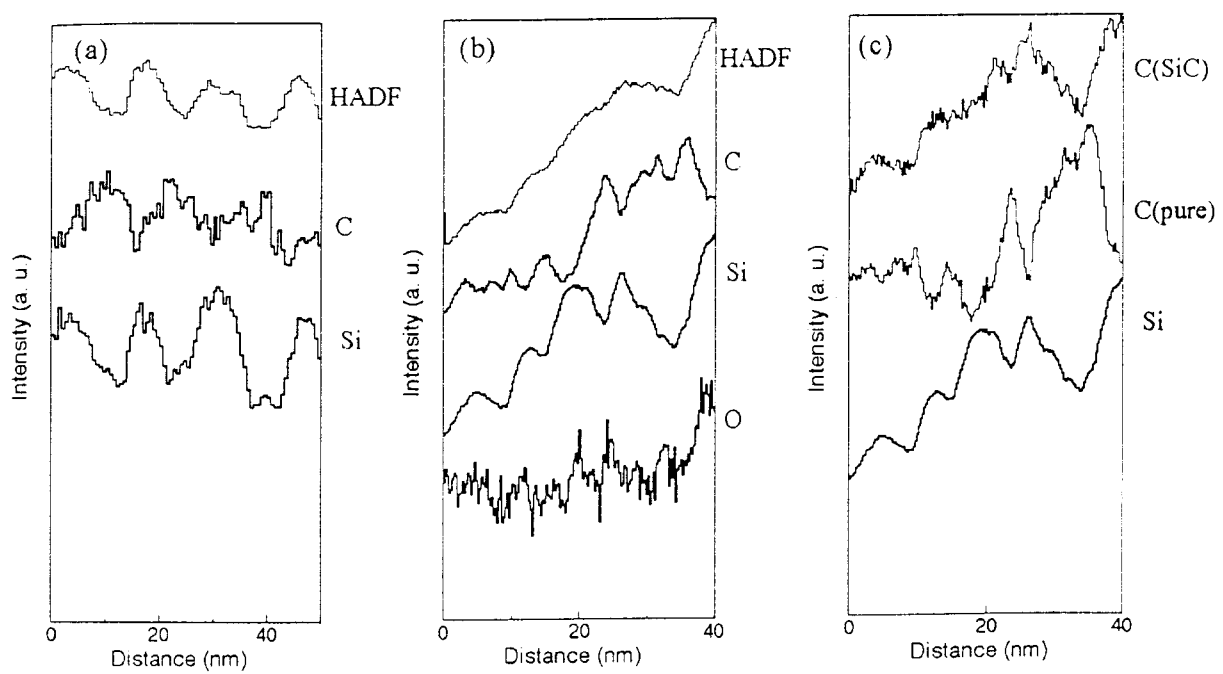


Fig. 7 EELS profiles for PCS-13 (a) and for PCS10-13 (b, c). (c): carbon ELNES profiles.